

PERFORMANCE BENEFITS OF SPHERICAL DIFFRACTING ARRAYS VERSUS FREE FIELD ARRAYS

Philip Gillett, Marty Johnson, and Jamie Carneal

Vibration and Acoustic Laboratories
Department of Mechanical Engineering
Virginia Tech

ABSTRACT

There are applications where microphone arrays must be integrated into/onto a structure. As an example there are efforts to instrument soldiers' helmets and vehicles with sensors in order to detect and localize noise events. In these cases the sound will be diffracted around the support platform. In this paper a spherical diffracting platform is used and is shown to improve low frequency performance. The sphere was chosen as its diffraction can be modeled analytically and it is similar to a helmet. Specifically, this paper will compare both theoretical and experimental results for spherical free field and diffracting arrays of identical geometries to examine the effect diffraction has on the array performance. Singular values of the array manifold matrix will be compared to show that diffracting arrays outperform free field arrays, especially at lower frequencies.

Index Terms— Acoustic diffraction, Acoustic signal processing, Acoustic arrays, Diffraction, Source location

1 INTRODUCTION

This paper is concerned with the performance of a nominally spherical microphone array mounted on a diffracting body. The reason for this design choice is two-fold. First, spherical arrays, unlike line or planar arrays, have beam patterns that are similar in all directions and are therefore not biased to any particular orientation between the source and the array. Secondly, the intention is to embed the microphone arrays into hard pre-existing structures such as helmets (see Figure 1a). These arrays are intended to act as nodes in a multinode dynamic network [1] for passive surveillance and tracking where the orientation between the source and array is not known a priori. Examples of spherical array geometries have been shown to accurately measure sound fields, both when in the free field [2], and mounted on a rigid sphere [3]. Furthermore, the presence of a rigid sphere as a mounting surface has been shown to increase low frequency beamforming performance [4]. This paper will focus on a hemispherical array mounted on a

rigid sphere (see Figure 1b) and will compare the results with a geometrically identical array acting in a free field (i.e. no diffracting body). This extends previous work on a microphone array placed on a rigid cylinder [5,6] where it was shown that there are substantial performance benefits using the diffracting body, especially at low frequencies. As this work will be extended to include non-symmetrical shapes, such as the helmet shown in

Figure 1, it becomes difficult to find simple analytical models to determine the array manifolds (magnitude and phase differences at the microphones due to array geometry and diffraction) and either computationally intensive numerical models [7] or an experimental approach is required. For this work an experimental approach using a source and reference microphone in an anechoic environment is used to verify the theory [5].

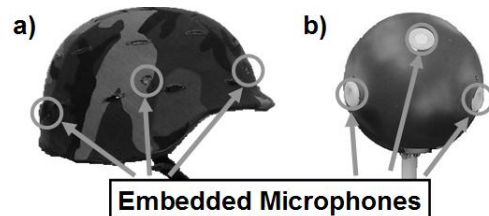


Figure 1. a) Helmet mounted array and b) spherical array used for this work.

2 THEORY: SOUND SOURCE LOCALIZATION

The goal is to accurately estimate an angle of arrival of the noise source relative to the microphone array using the measured set of microphone signals. The outputs from a number of arrays can then be fused together in order to estimate the location of the source in space. In order to achieve this a Minimum Variance Distortionless Response (MVDR) beamformer is used.

Let X be a complex vector of microphone responses at frequency ω and Y be the beamformed output. There exists a set of complex weights w_θ that preserves the power in the look direction θ while minimizing the power of the output signal Y [8]:

$$Y = w_\theta^H X \quad \text{Eq. 1}$$

$$w_\theta^H d_\theta = 1 \quad \text{Eq. 2}$$

$$\min w_\theta^H \Phi_{\text{xx}} w_\theta \quad \text{Eq. 3}$$

where H indicates the Hermitian transpose, d_θ is the array manifold vector of the array in the look direction θ , and Φ_{xx} is the cross spectral density (CSD) matrix for the microphone inputs and is based on an assumed noise model. The MVDR filters are then calculated by:

$$w_\theta = \frac{\Phi_{\text{xx}}^{-1} d_\theta}{d_\theta^H \Phi_{\text{xx}} d_\theta} \quad \text{Eq. 4}$$

Different look directions (or choices of θ) can then be chosen to build up an array of beamformer weights for the various look directions of interest. The critical point here is that if Φ_{xx} is ill-conditioned, which is typically the case at low frequencies, then the matrix must be conditioned before inversion. Diagonal loading is one such conditioning technique:

$$w_\theta = \frac{\Phi_{\text{xx}} + \alpha \mathbf{I} d_\theta}{d_\theta^H (\Phi_{\text{xx}} + \alpha \mathbf{I}) d_\theta} \quad \text{Eq. 5}$$

where α is a conditioning term and \mathbf{I} is the identity matrix. For these ill-conditioned cases there is a basic tradeoff between accurate localization (or *Directivity Index*) and sensitivity to sensor noise (or *White Noise Gain*) [6]. As the coefficient α is increased the white noise gain improves at the cost of poor directivity. In this paper the normalized singular values of the CSD matrices will be investigated as a measure of overall performance of each array. As a simple rule, the larger the singular values at a frequency, the better the conditioning and hence the better the localization performance of the array for a given white noise gain [6]. The model used here will assume a diffuse noise field where the CSD matrix can be estimated directly from the array manifold matrix \mathbf{D} (and is described in more detail in reference [6]). The array manifold matrix is the set of M microphone responses to unit plane waves in L directions. The number of directions chosen depends upon the spatial sampling strategy employed, whether based on equal angles, equal areas, etc.

$$\Phi_{\text{xx}} = \mathbf{D} \mathbf{B} \mathbf{D}^H \quad \text{Eq. 6}$$

\mathbf{D} has dimensions of number of sensors by number of look angles (i.e. the manifold vector d_θ for look direction θ occupies a single column of the matrix) and \mathbf{B} is a diagonal matrix of weights. The diffuse field model assumes that the noise field is generated by incoherent noise sources acting equally from all angles and therefore \mathbf{B} is chosen to maintain this equal power from equal area assumption if the look angles are not equally spaced.

2.1 Finding Array Manifolds

The calculation of the MVDR filters requires measurements or estimates of the array manifold matrix \mathbf{D} . In this paper, four sets of array manifolds will be estimated and compared: (i) theoretical free field array calculated using the free-field wave equation, (ii) theoretical diffracting array calculated using spherical harmonic diffraction [9], (iii) experimentally measured free-field array and (iv) experimentally measured diffracting array. It is beyond the scope of this paper to describe the theoretical calculation of diffraction due to a sphere and the reader is referred to the literature for more details.

If the array is small as compared to the distance from the source (plane wave assumption) then the normalized free-field manifolds can be calculated as,

$$d_\theta = e^{-jkr_\theta} \quad \text{Eq. 7}$$

where k is the wavenumber given by the frequency divided by the speed of sound and r_θ is a vector of path length differences $[r_1, r_2, \dots]^T$ from the individual array elements to the source at angle θ as shown in Figure 2.

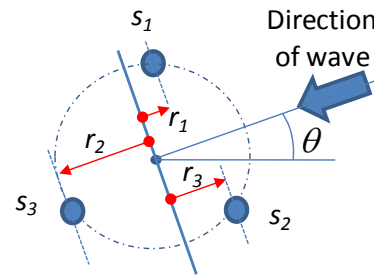


Figure 2: Relative path length differences for a three element array with wave arriving at angle θ

3 EXPERIMENTS

3.1 Experimental Setup

The diffracting array was constructed from a 0.26m diameter rigid plastic sphere with three microphones placed at the equator at azimuth angles of 0° , 120° , and 240° , and three microphones placed at 35° elevation from horizontal at azimuth angles of 60° , 180° , and 300° . The microphone array itself was mounted on a wire mesh that fit tightly over the rigid sphere. This mesh was easily removable so that a comparison between identical geometries could be performed with and without the diffracting body. The array was placed in an anechoic chamber and the array manifold was measured at 15° azimuth angle increments and 20° elevation angle increments from 0° to 80° elevation using a speaker as a sound source (see [5] for more details). This resulted in a $[6 \times 120]$ manifold matrix of the form [number of microphones by number of directions] for a range of frequencies 0-4KHz for both the diffracting and the non-diffracting arrays. An examination of spatial sampling methods is presented by Rafaely [10], and the non-uniform

spacing chosen here was based on experimental apparatus constraints.

The matrix \mathbf{B} (Eq. 6) must be used to account for the relatively coarse sampling near the equator and very dense sampling near the poles. Therefore b_{ii} , the i^{th} diagonal element of \mathbf{B} corresponding to the i^{th} angle, is weighted in proportion to the cosine of its elevation angle ϕ_i .

$$b_{ii} = \cos(\phi_i) \quad \text{Eq. 8}$$

The geometry of the array was chosen to mirror what could be equipped in a real world system on a diffracting body such as a helmet, with an example shown in

Figure 1. Sampling only the upper hemisphere of directions was also chosen based on real world testing, where arrays are placed on the surface of the earth and sound sources are typically never below that surface. Alternative geometries can be chosen without changing the basic methodology and conclusions of this paper.

3.2 Results

A tradeoff when designing microphone arrays is the spacing of sensors and the effective frequency range of the array. The dimensions of an array placed on a helmet would normally predispose it to poor low frequency performance, but the presence of the rigid helmet mitigates this problem. One way of viewing the beamforming and localization ability of an array is to examine the normalized singular values of its CSD matrix. At each frequency, the relative magnitude of each singular value, normalized to the largest singular value, indicates how well conditioned the CSD matrix is. The ability of an array to beamform or localize at a particular frequency is based on the phase differences between array elements. When the wavelength with respect to the array size is very large, there is effectively no phase difference between microphones, creating a poorly conditioned CSD matrix and poor performance. The trend is seen in the singular values of the CSD matrix at low frequencies, where the largest singular value is relatively dominant, indicating that the array size is too small to effectively beamform. The main point of examining the singular values of the CSD matrix is that any localization or beamforming algorithm that relies on phase differences between array elements will be affected.

The singular values for a theoretical free field array and a theoretical diffracting array are shown in Figure 3 over the frequency range 100-4000Hz. In both cases the maximum singular value has been normalized to 0dB. The next two lines for each array both represent two singular values (the lines fall on top of one another due to symmetry). It is clear that at any given frequency the singular values for the diffracting array are larger than the non-diffracting array, leading to better localization performance for a given white noise gain. The next comparison, shown in Figure 4, is between experimental and theoretical results for a free field array and shows a very high degree of agreement. Any variations between the results could be due to slight errors in

the position of the microphones. This validates the experimental procedure used to measure \mathbf{D} .

Figure 5 shows a comparison between experimental and theoretical results for the diffracting case. As in the case of Figure 4, good agreement is found between measured and theoretical data. The last comparison made is between measured free field and measured diffracting CSD matrices, shown in Figure 6. The most important feature to note in Figure 6 is how the singular values for the diffracting array are consistently larger than the singular values for the free field array at frequencies below 1000 Hz. The increase in singular values at low frequencies translates to an increase in localization performance.

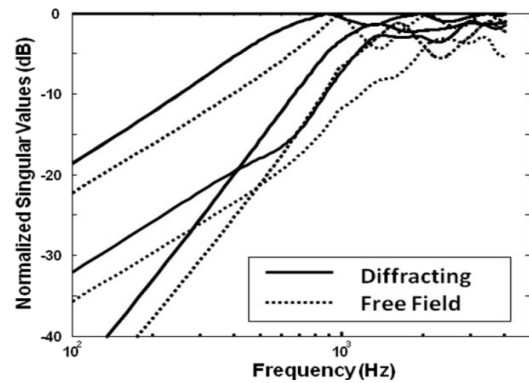


Figure 3. Singular values for diffracting and free field spherical arrays of identical geometries using theory.

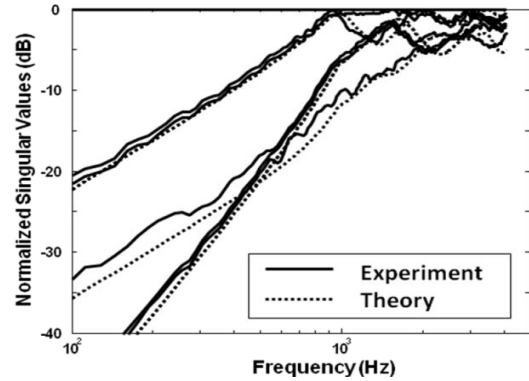


Figure 4. Singular values for free field spherical arrays using measurements and theory.

When viewing Figure 3 through Figure 6, the relative magnitude of the singular values are important based on the conditioning of the CSD matrix necessary to allow the matrix inversion of equation 6. The impact of conditioning is similar to ignoring singular values below some value, proportional to α . As an example, assume the conditioning is such that the value is -10dB. Referring to Figure 6, the diffracting array has 3 singular values above -10dB at 300 Hz, whereas the free field array has only 1. This results in better performance at lower frequencies for the diffracting array compared to the free field array.

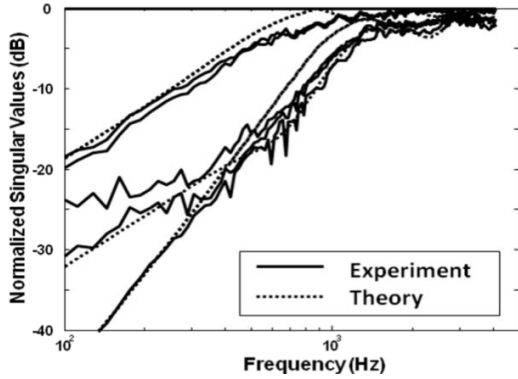


Figure 5. Singular values for diffracting spherical arrays using measurements and theory.

One explanation as to why the singular values for the diffracting array are consistently higher than those values for the free field array is the increased phase difference between array elements [11]. The presence of a rigid body allows the phase to develop as the wavefront diffracts around it. To illustrate, Figure 7 shows the maximum phase measured by the array at an azimuth angle of 0° and an elevation angle of 0° for a frequency range of 50 to 500 Hz.

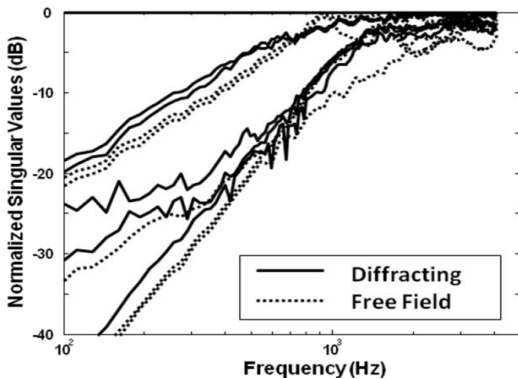


Figure 6. Singular values for diffracting and free field spherical arrays using measurements.

4 CONCLUSIONS

An overview of a simple localization method using MVDR filters has been presented which uses diagonal loading to condition the CSD matrix. Theoretical results for both diffracting and free field arrays have been compared to show that the singular value magnitudes of diffracting arrays are consistently larger than the values of free field arrays. Experimental results have been compared to theoretical results to show good agreement between measurements and theory. A final comparison using experimental results for diffracting and free field arrays was presented to show a performance benefit represented by larger singular values at lower frequencies. Lastly, a simple explanation for the origin of large singular values was given based on the maximum phase difference that each microphone array experiences.

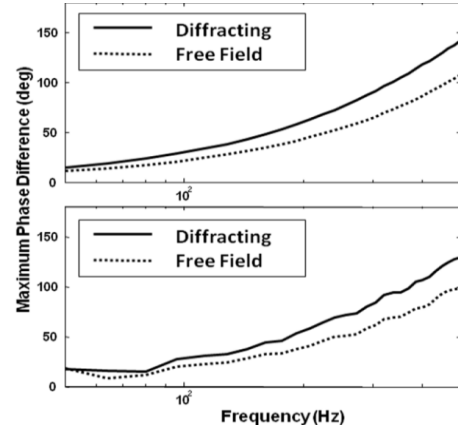


Figure 7. Maximum phase difference between microphones at an azimuth angle of 0° and an elevation angle of 0° for theoretical (UPPER) and experimental results (LOWER).

5 REFERENCES

- [1] D. Mennitt, P. Gillett, J. Carneal and M. Johnson, "Noise Source Tracking Using Multiple Diffracting Arrays," ACTIVE 2006, Adelaide Australia, Sept 2006
- [2] T.D. Abhayapala and D.B. Ward, "Theory and design of high order sound field microphones using spherical microphone array," in *Proc. ICASSP*, vol 2, 2002, pp. 1949-1952.
- [3] M. Park and B. Rafaely, "Sound-field analysis by plane wave decomposition using spherical microphone array," *J. Acoust. Soc. Am.* **118**, Nov. 2005, pp.3094-3103.
- [4] J. Meyer, "Beamforming for a circular microphone array mounted on spherically shaped objects," *J. Acoust. Soc. Am.* **109**, Jan. 2001, pp. 185-193.
- [5] M. Johnson, J. Carneal, and P. Gillett, "Comparison of a diffracting and a non-diffracting circular acoustic array," in *Proc. ICASSP*, vol. 4, 2006, pp. 1081-1084, 2006
- [6] M. Johnson, J. Carneal and P. Gillett, "Comparison of a Diffracting and a Non-Diffracting Cylindrical Microphone Array," Proceedings of the Thirteenth International Congress on Sound and Vibration, Vienna, Austria, July 2006
- [7] P. Gillett, M. Johnson, and J. Carneal, "A computational model for optimizing microphone placement on headset mounted arrays," Invited Paper: 123rd Convention of the Audio Engineering Society, October 2007, New York, NY
- [8] J. Bitzer and K. Uwe Simmer, "Superdirective Microphone Arrays," in *Microphone Arrays*, M. Brandstein and D. B.Ward, Springer-Verlag, New York, pp. 19-38, 2001.
- [9] J. J. Bowman, T. B. A. Senior, and P. L. E. Uslenghi, *Electromagnetic and Acoustic Scattering by Simple Shapes* (North-Holland, Amsterdam), 1987.
- [10] B. Rafaely, "Analysis and design of spherical microphone arrays," *IEEE Trans. Speech and Audio Processing*, vol. 13, pp. 135-143, Jan. 2005.
- [11] G.A. Daigle, M.R. Stinson, and J.G. Ryan, "Beamforming with air-coupled surface waves around a sphere and circular cylinder," *J. Acoust. Soc. Am.* **117**, pp. 3373-3376, June 2005.